

Topic 2 : Diffraction

2.1 Introduction

So far we have considered a range of models for light, each one appropriate to the phenomena we are considering. The models so far have always taken the direction of the propagation to be given by Snell's Law, so that it only changes at refractive index boundaries.

To go further we need to consider the spatial wave nature of light, which results in diffraction. In this course we will consider a simplified scalar model where we will ignore the polarisation effects of light.

Consider an ideal *point source* where wave of wavelength λ spread out in three-dimensions from the point $(0, 0, 0)$ drawn from the y/z plane in figure 1.

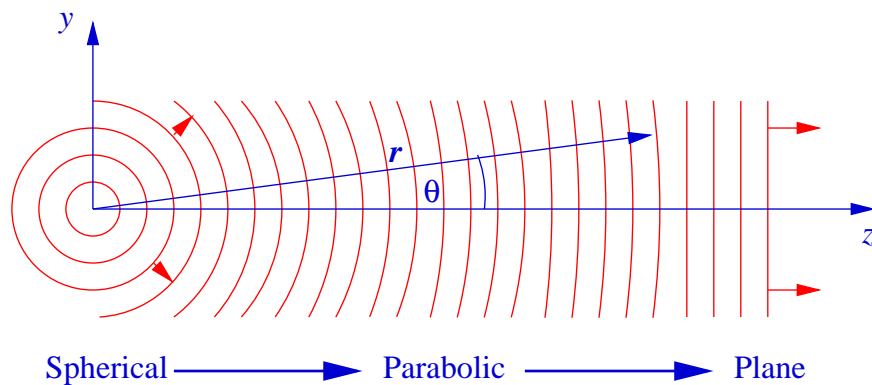


Figure 1: Spherical wave spreading from a point source.

Ignoring the time varying part, the *scalar amplitude* at a point a distance r from the origin is,

$$E(x, y, z) = \frac{E_0}{r} \cos(\kappa r) \quad \text{where } \kappa = \frac{2\pi}{\lambda}$$

and

$$r^2 = x^2 + y^2 + z^2 \quad \text{so that} \quad r = z \left(1 + \frac{x^2 + y^2}{z^2} \right)^{\frac{1}{2}}$$

with the intensity given by

$$I(r) = \frac{1}{2} |E(r)|^2 = \frac{1}{2r^2} |E_0|^2 = \frac{1}{r^2} I_0$$

which is *inverse square* relation, so the apparent intensity of the source drops off as the square of the distance.

When *very close* to the point source, we have to use the full expression for r which corresponds to *spherical expanding* waves, however as z becomes large we can start taking approximations that simplify the calculations.

Parabolic Approximation:

If $z \ll x/y$, we can expand the expression for r to give



$$r = z + \frac{x^2 + y^2}{2z}$$

which corresponds to parabolic wave approximation, which will result in *Fresnel* or *near field* diffraction.



Plane Wave Approximation:

The further approximation is that the wavefronts are *locally plane* as shown in figure 2.

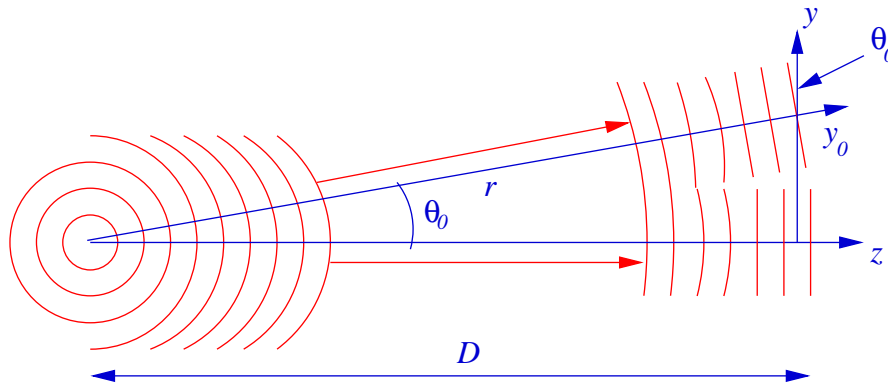


Figure 2: Far field approximation from a point source.

At a distance D from the point source at angle θ_0 , then about the the point y_0 , we have that

$$r = \frac{D}{\cos \theta_0} + (y - y_0) \sin \theta_0 \quad \text{where} \quad y_0 = D \tan \theta_0$$

This approximation is equivalent in expressing the wavefront as a series of *plane waves*, which will result in *Far Field* diffraction. As we will see this apparently rather drastic approximation results in many more usable results than you would expect.

In this course we will only deal with *far field* diffraction, which can be formulated in a Fourier scheme. This will allow us to understand the effects of diffraction on imaging systems.



2.2 Far Field Diffraction from a Single Slit

Consider a single slit of width d in plane P_0 being illuminated by a scalar wave of wavelength λ . In plane P_1 a *large* distance D along the z axis, we consider a point s as shown in figure 3, where the line from the centre of the slit to s makes an angle θ with the z axis.

If we assume that $D \gg d$ the width of the slit, then angle of the rays (a) from the *top* of the slit, and (b) from the *bottom*, to s is also θ , then, as seen from s there appears to be a phase shift $\delta(y)$ across the slit given by

$$\delta(y) = \kappa y \sin \theta \quad \text{where} \quad \kappa = \frac{2\pi}{\lambda}$$

The distance R from the slit to the point s can also be taken as constant, being,

$$R = \frac{D}{\cos \theta}$$

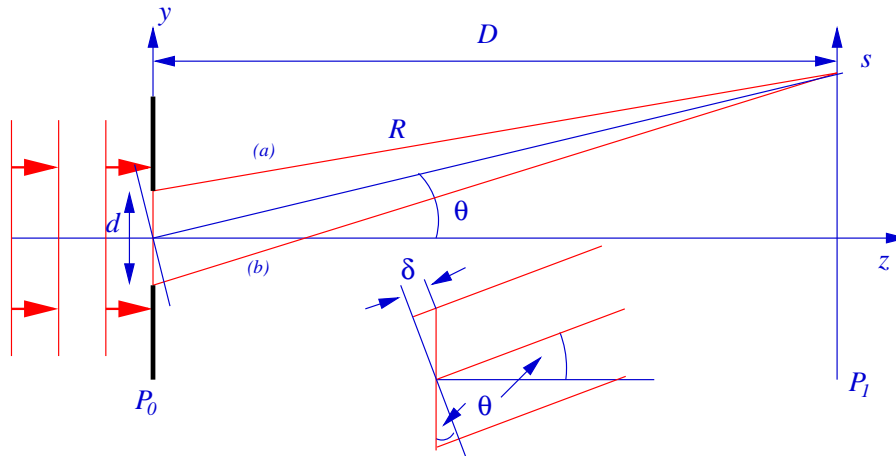


Figure 3: Layout and construction for far-field diffraction from a single slit

The scalar amplitude at s will then be a summation of the components coming from the slit, so will be,

$$E(\theta) = \frac{E_0}{R} \int_{-d/2}^{d/2} \cos(\kappa y \sin \theta) dy$$

where E_0 is the scalar amplitude at the slit. This can be integrated to give

$$E(\theta) = \frac{E_0}{R \kappa \sin \theta} \left| \sin(\kappa y \sin \theta) \right|_{-d/2}^{d/2} = \frac{2E_0 \sin\left(\frac{\kappa d}{2} \sin \theta\right)}{R \kappa \sin \theta}$$

To simplify this expression let

$$\beta = \frac{\kappa d}{2} \sin \theta = \frac{\pi d}{\lambda} \sin \theta$$

we can then write $E(\theta)$ as

$$E(\theta) = \frac{E_0 d \sin \beta}{R \beta}$$

The intensity, which is what we would actually measure, is now given by

$$I(\theta) = \frac{1}{2} |E(\theta)|^2 = I_p \left(\frac{\sin \beta}{\beta} \right)^2 = I_p \text{sinc}^2 \beta \quad \text{where} \quad I_p = I_0 \frac{d^2}{R^2}$$

where I_0 is the intensity at the slit, being $I_0 = \frac{1}{2} |E_0|^2$. For *small* θ , the shape of this function is dominated by the $\text{sinc}^2 \beta$ term, which is plotted in figure 4.

The $\text{sinc}^2 \beta$ term is zero for $\beta = \pm m \pi$, giving zeros of the pattern when

$$\sin \theta_m = \frac{m \lambda}{d} \quad \text{for } m = \pm 1, \pm 2, \pm 3, \dots$$



This gives the angular shape of the diffracted pattern when $D \gg d$.

2.3 Diffraction Pattern from Slit and Lens

The above formulation assumes that the diffracted wavefronts after the slit are plane which result on diffraction pattern formed at *infinity*. A more useful geometry is to have a slit of width d immediately followed by a lens of focal length f as shown in figure 5.

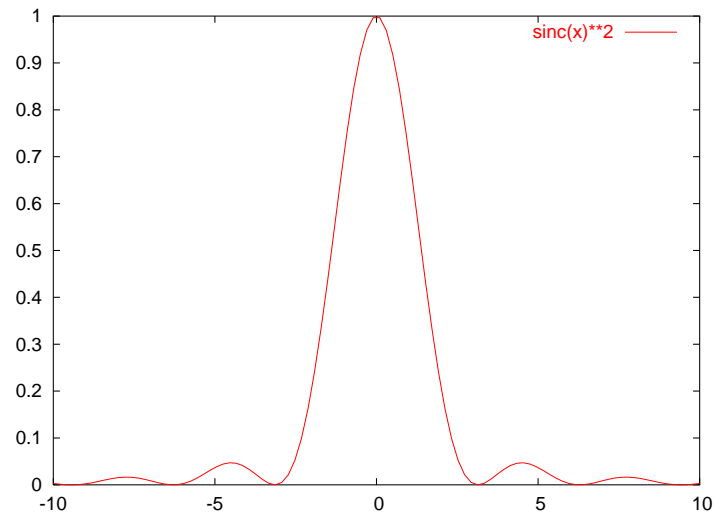


Figure 4: Shape of $\text{sinc}^2(x)$

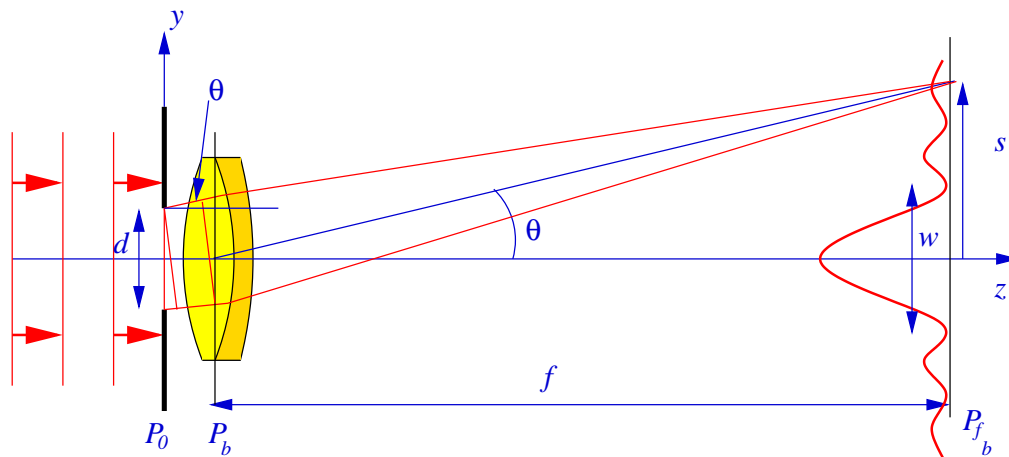


Figure 5: Diffraction from a slit imaged by a lens

We know from previous that a collimated beam at angle θ striking the front of the lens are images to a point in the back focal plane P_{f_b} , which is a distance f from the back principal plane of the lens. Thus a plane wave, diffracted in direction θ will be focused as s , where

$$s = f \tan \theta \approx f \theta \quad \text{for small } \theta$$

so the intensity in the back focal plane will be,

$$I(s) = I_p \text{sinc}^2 \left(\frac{\pi d}{\lambda f} s \right)$$



which has zeros at

$$s_m = m \frac{\lambda f}{d} \quad \text{for } m = \pm 1, \pm 2, \pm 3, \dots$$

so having a *width*, being the distance between the ± 1 zeros, of

$$w = \frac{2 \lambda f}{d}$$

Note the reciprocal relations between d and w , as as the slit get *narrower* then it diffraction pattern gets *wider*.

2.4 The Fourier Approach

The Fourier transform¹ of a function $f(x)$ is given by,

$$F(u) = \mathcal{F}\{f(x)\} = \int_{-\infty}^{\infty} f(x) \exp(-i 2\pi ux) dx$$



which for a real function $f(x)$ we can write as

$$F(u) = \int_{-\infty}^{\infty} f(x) \cos(2\pi ux) dx - i \int_{-\infty}^{\infty} f(x) \sin(2\pi ux) dx$$

If we now define a function $p(x)$ which represents the *slit* being,

$$\begin{aligned} p(x) &= 1 \quad \text{for } |x| < d/2 \\ &= 0 \quad \text{else} \end{aligned}$$

then from previous we can write that,

$$E(\theta) = \frac{E_0}{R} \int_{-\infty}^{\infty} p(y) \cos(\kappa y \sin \theta) dy = \frac{E_0}{R} \mathcal{R}\{P(\kappa \sin \theta)\} \quad \text{where } \kappa = \frac{2\pi}{\lambda}$$

where $P(u) = \mathcal{F}\{p(x)\}$, or more importantly, if we have a lens of focal length f after the slit, then in the back focal plane of the lens we have

$$E(s) = \frac{E_0}{f} \int_{-\infty}^{\infty} p(y) \cos\left(\frac{2\pi}{\lambda f} ys\right) dy = \frac{E_0}{f} \mathcal{R}\left\{P\left(\frac{1}{\lambda f} s\right)\right\}$$

and the intensity,

$$I(s) = I_0 \left| P\left(\frac{s}{\lambda f}\right) \right|^2$$



so we have the important result that the intensity in the back focal plane is the modulus squared of the *scaled* Fourier transform of $p(x)$, which represents the *slit*. It is easy to show that $\mathcal{F}\{p(x)\}$ is given by

$$P(u) = d \operatorname{sinc}(\pi d u)$$

where d is the the width of the slit.

The scheme is easily extended to a two-dimensional *slit*, being a *rectangle* of sides $a \times b$, by defining a rectangle function,

$$\begin{aligned} p(x, y) &= 1 \quad \text{when } |x| < a/2 \text{ and } |y| < b/2 \\ &= 0 \quad \text{else} \end{aligned}$$

The two-dimensional Fourier transform is given by

$$P(u, v) = a b \operatorname{sinc}(\pi a u) \operatorname{sinc}(\pi b v)$$

¹See The Fourier Transform, (What you need to know), for detail.

since both the Fourier transform and $p(x, y)$ is separable. Then following the above scheme the intensity diffracted from a rectangle, in the back focal plane of a lens of focal length f is given by

$$I(s, t) = I_0 \operatorname{sinc}^2\left(\frac{\pi a s}{\lambda f}\right) \operatorname{sinc}^2\left(\frac{\pi b t}{\lambda f}\right)$$

where I_0 is the intensity at the centre of the pattern. This shape is plotted as a surface plot in figure 6, for for an aperture where $a = 3b$ showing two sinc^2 at right angles, one being the three times wider than the other. The $\log()$ of the function is also plotted which makes the structure much more obvious.

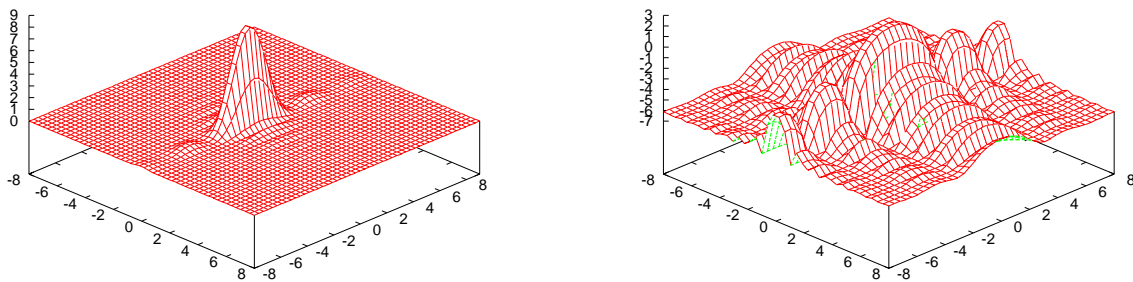


Figure 6: Plot of diffraction pattern from a rectangular aperture with of size $a \times b$ where $a = 3b$, and its $\log()$.

2.5 Diffraction from Two Slits

The power of the Fourier approach really become obvious when the diffracting object become more complex. Consider diffraction from *two* slits of width a separated by b . If, as above, we define $p(x)$ to be the transmission function for one slit, being given by

$$\begin{aligned} p(x) &= 1 \quad \text{for } |x| < a/2 \\ &= 0 \quad \text{else} \end{aligned}$$

then *two* slits, separated by b can be written as

$$f(x) = p(x) \odot \left[\delta\left(x - \frac{b}{2}\right) + \delta\left(x + \frac{b}{2}\right) \right]$$

where $\delta(x)$ is the δ -function, and \odot is the convolution operator. This is shown schematically in figure 7.

We then know from the *convolution theorem*, that the Fourier transform is just the product of the Fourier transform of the two function, so in this case we get that

$$F(u) = \operatorname{sinc}(\pi a u) \cos(\pi b u)$$



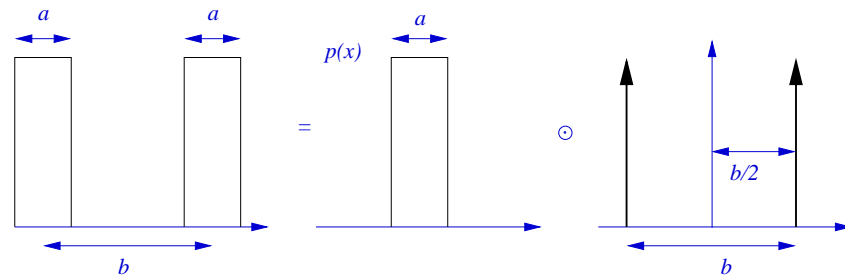



Figure 7: Representation of two slits by convolution.

The diffracted intensity behind a lens of focal length f is now just

$$I(s) = I_0 \operatorname{sinc}^2\left(\frac{\pi a}{\lambda f} s\right) \cos^2\left(\frac{\pi b}{\lambda f} s\right)$$

 where I_0 is the intensity at the centre of the pattern. A plot of this intensity for $b = 6a$ is shown in figure 8, along with a $\log()$ plot to make the outer peaks more visible.

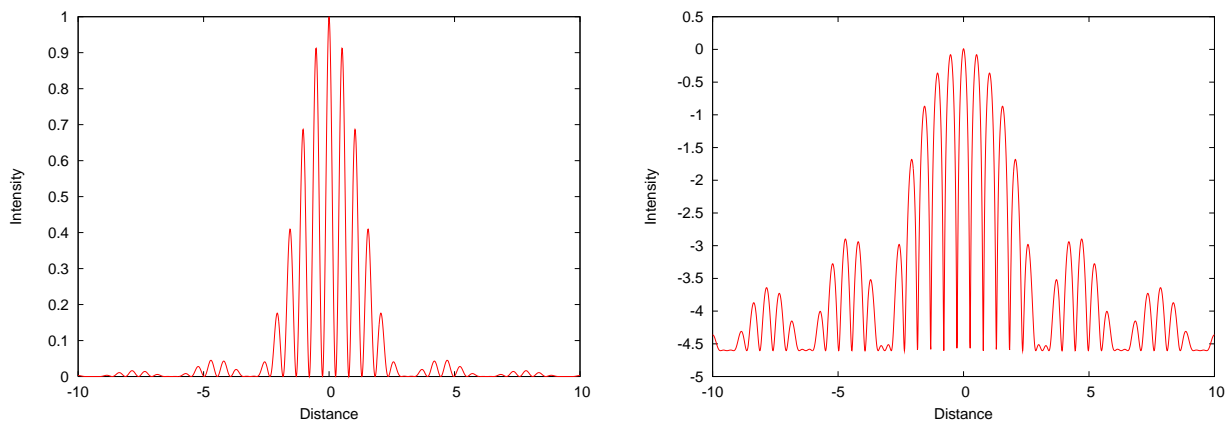


Figure 8: Plot of intensity diffracted from two slits separated by *six* times their width, and its $\log()$.

The shape is $\cos()$ fringes from the two slits, exactly as seen in workshop question 7.1, but modulated by the $\operatorname{sinc}^2()$ resulting from the finite thickness of the slits. If you compare this analysis with the traditional scheme in the textbooks, the power of the Fourier techniques is obvious!

2.6 The Diffraction Grating

The diffraction grating is a series of *thin* slits all separated by a distance d , which is imaged by a lens of focal length f as shown in figure 9. The traditional and simple analysis is that at angle θ , the phase delay between light diffracted from adjacent slits is,

$$\delta = \frac{2\pi}{\lambda} d \sin\theta$$

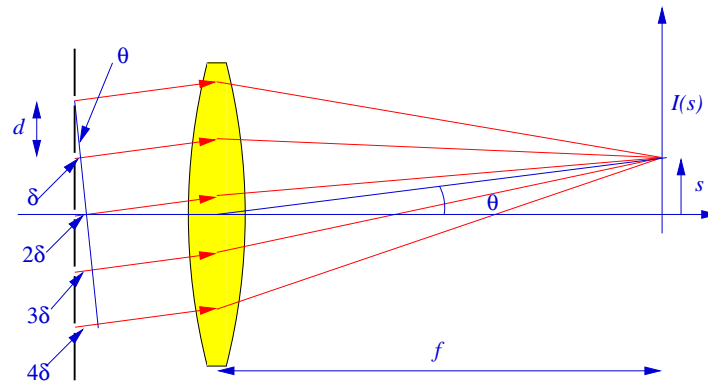


Figure 9: Diffraction grating images by a lens.

so there will all sum together coherently, when

$$\delta = 2 m \pi$$

so giving a series of *peaks* when

$$d \sin \theta_m = m \lambda \quad \text{for } m = 0, \pm 1, \pm 2, \dots$$



In the back focal plane of a lens of focal length f which, for *small* θ , will give a series of peaks at,

$$s_m = m \frac{\lambda f}{d} \quad \text{for } m = 0, \pm 1, \pm 2, \dots$$

However this does not tell us anything about the shape of the peaks, or what happens when the slits are of finite width, for this we need Fourier methods.

We can represent a series of *very thin* slits by a series of δ -functions, each separated by distance d , by

$$c(x) = \sum_{m=-\infty}^{\infty} \delta(x - m d)$$

which is the Comb() function as shown in figure 10. Its Fourier transform is also a Comb(), but of reciprocal spacing, so

$$C(u) = \sum_{m=-\infty}^{\infty} \delta\left(u - \frac{m}{d}\right)$$



The intensity output behind a lens of focal length f is then given by

$$I(s) = I_0 \left| C\left(\frac{s}{\lambda f}\right) \right|^2$$

which is just a set of δ -functions located at

$$s_m = m \frac{\lambda f}{d} \quad \text{for } m = 0, \pm 1, \pm 2 \dots$$

which is identical to the *first principals* analysis.

Consider a full description of a grating with period d , slit width a , and finite length $D = N d$, as shown in figure 11. Using the notation in the figure, then the grating can

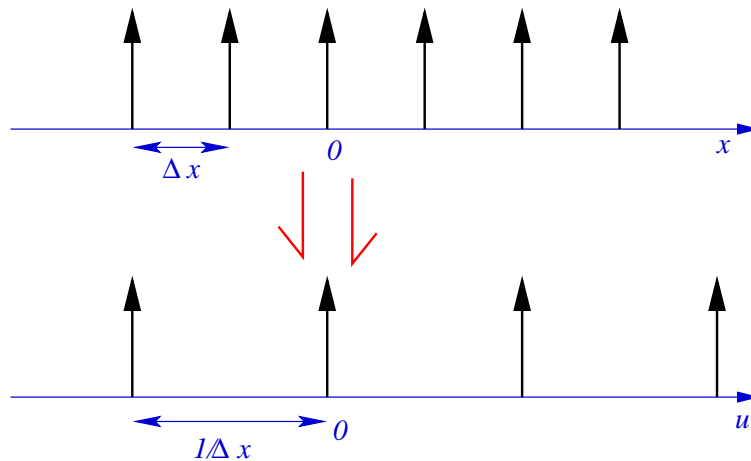


Figure 10: A Comb() function and its Fourier Transform.

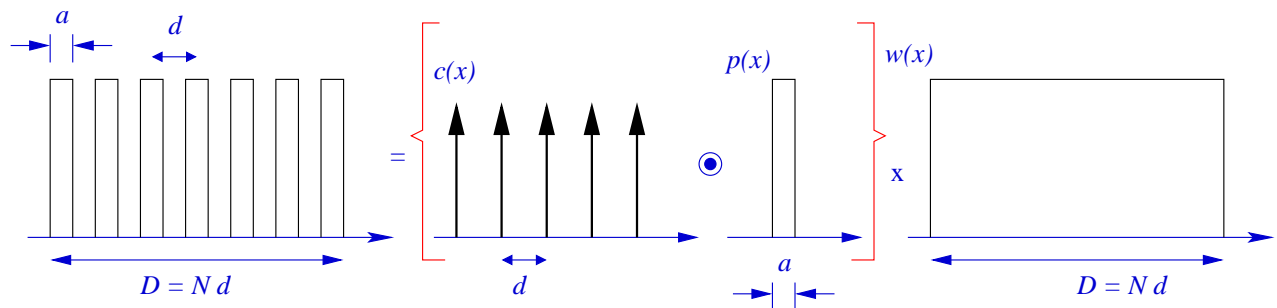


Figure 11: Full description of a grating of period d , slit width a and finite extend $D = Nd$

be described by a function,

$$f(x) = \{c(x) \odot p(x)\} w(x)$$



which again from the *convolution theorem*, has Fourier transform

$$F(u) = \{W(u) \odot C(u)\} P(u)$$

where

$$C(u) = \sum_{m=-\infty}^{\infty} \delta\left(u - \frac{m}{d}\right) \quad , \quad P(u) = \text{sinc}(\pi a u) \quad \text{and} \quad W(u) = \text{sinc}(\pi N d u)$$

The intensity is then just,

$$I(s) = I_0 \left| F\left(\frac{s}{\lambda f}\right) \right|^2$$



which is plotted for $a = 1$, $d = 5$ and $N = 10$, which shows a series of sharp $\text{sinc}^2()$ functions separated by a constant distance and weighted by an overall $\text{sinc}^2()$.

2.6.1 The Grating Spectrometer

In the grating spectrometer a collimated beam containing multiple wavelengths strikes a diffraction grating and is diffracted to form \pm -order diffracted spectra as shown in

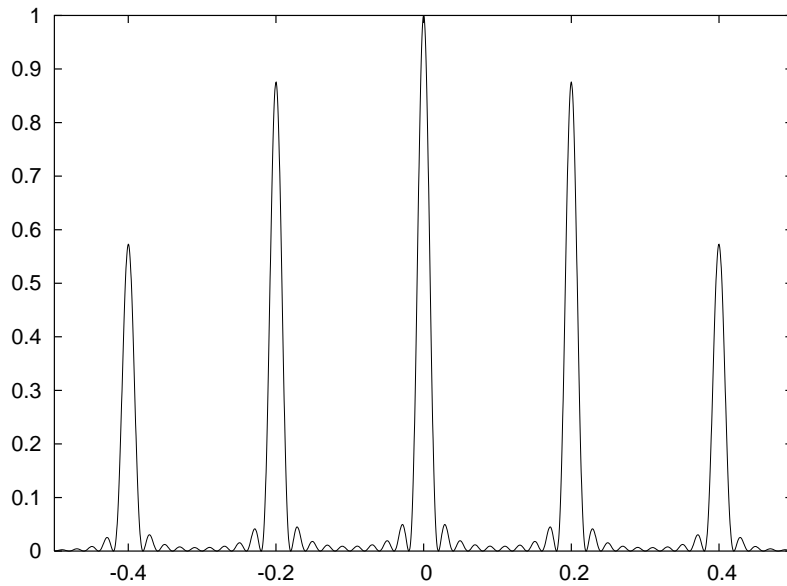


Figure 12: Output of a grating of period d , slit width a and finite extend $D = Nd$

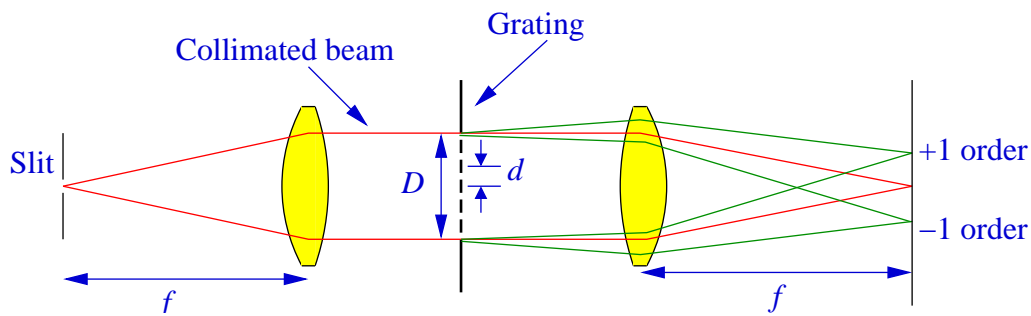


Figure 13: Layout of basic grating spectrometer.

figure 13. In practical systems the imaging lens system can rotate about the centre of the grating so that the angle of the diffracted image of the slit can be measured.

Consider the system being illuminated with two wavelength λ_1 and λ_2 , then at the m^{th} order diffraction pattern we two $\text{sinc}^2()$ peaks as shown in figure 14. This position of the centre of the two peaks will be at

$$s_1 = \frac{m \lambda_1 f}{d} \quad \text{and} \quad s_2 = \frac{m \lambda_2 f}{d}$$

where d is the grating spacing, and f is the effective focal length of the spectrometer imaging system. Their separation will therefore be

$$\delta s = \frac{m \delta \lambda f}{d} \quad \text{where} \quad \delta \lambda = \lambda_1 - \lambda_2$$

Each peak is a $\text{sinc}^2()$, and if we assume that $\lambda_1 \approx \lambda_2$ then both peaks have the same width, with their first zero at a distance

$$\Delta s = \frac{\lambda_0 f}{D} \quad \text{where} \quad \lambda_0 = \frac{1}{2}(\lambda_1 + \lambda_2)$$

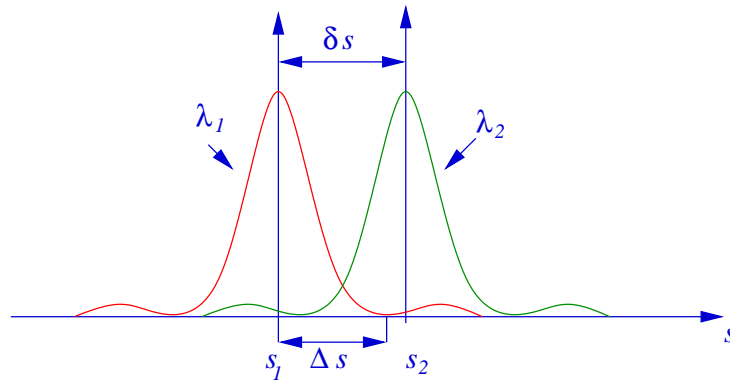


Figure 14: Diffraction from source with two wavelengths.

We get

1. $\delta\lambda$ is *large*, then $\delta s \gg \Delta s$, so the two peaks are *well separated*, and hence *resolved*,
2. $\delta\lambda$ is *small* the two peaks start to overlap, and finally merge to one as $\delta\lambda \rightarrow 0$, and hence *not resolved*.

We say that the two peaks are *just resolved* when $\delta s = \Delta s$, so that the centre of one peak is at the first zero of the other. This is shown in figure 15, showing at this criteria there is a *valley* of about 20% of the peak height.

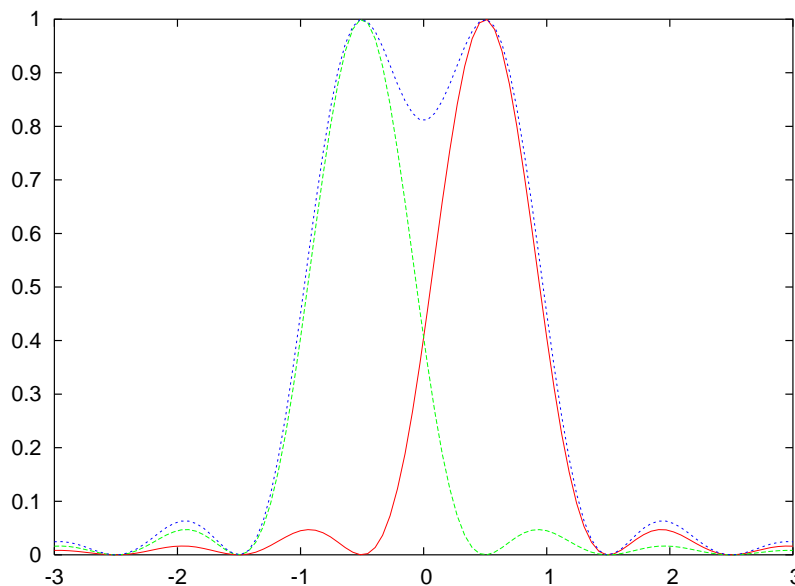


Figure 15: Two $\text{sinc}^2()$ peaks at their resolution limit

This sets a limit of the smallest $\delta\lambda$ we can resolve with this instrument where

$$\frac{\lambda_0}{\delta\lambda} = \frac{mD}{d} = mN$$

where N is the number of lines on the grating, and λ_0 is the *average* wavelength and m is



the diffraction *order*. Therefore to get a good resolution we been a grating *large* grating with *many lines*, and ideally use as high an order as possible. See workshop question ?? for a numerical example.

2.7 Practical Diffraction Gratings

Most practical diffraction gratings for spectroscopic applications operate in *reflection* rather than transmission and are typically *blazed* as shown in figure 16 with *wedge* shaped grooves where γ is known as the *blaze angle*.

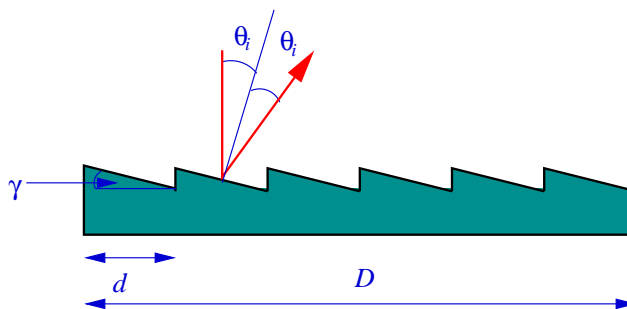


Figure 16: Profile of a blazed diffraction grating.

A vertical beam striking one wedge facet as shown, makes an angle θ_i to the surface normal and will be reflected at angle $2\theta_i$. Noting that $\theta_i = \gamma$ the blaze angle, then the specular reflection from this grating will be a angle 2γ which is the direction that most of the incident intensity will be directed. If we also arrange that the grating period, d is such that for a given wavelength λ_0 , and order m

$$\sin 2\gamma = \frac{m\lambda_0}{d}$$

then the specular reflection will be in the same direction as the m^{th} diffracted order, so most of the light will be in this order, and the other orders much reduces. This structure has no effect on the grating resolution, but significantly increases its light efficiency, so allowing analysis of lower intensity sources. This is of particular importance in astronomy where light from distant objects is very faint.

Traditionally grating made by mechanically cutting grooves is a nickel block which was then coated in silver to give a reflective grating. Modern gratings produced optically by photographically recording a high frequency interference pattern which is then chemical etched into a solid materials, often quartz, which is can either be left as a transmission grating of silver coated to give a reflection coating.

The *laboratory grade* gratings found in teaching spectrometers are formed by making a plastic contact replica of a master metal grating which is then bonded to a solid glass substrate. Again these may be silver or aluminum coated to form reflection gratings.

2.8 Diffraction from a Circular Aperture

As most optical systems are circular, the next most useful diffraction to consider is the *circular aperture*, which is going to give up the shape of the spot formed by a lens.

Consider the circular aperture of radius a , being defined by,

$$p(x, y) = \begin{cases} 1 & \text{when } x^2 + y^2 \leq a^2 \\ 0 & \text{else} \end{cases}$$



First we need to calculate the Fourier transform $P(u, v)$, which using

$$x = \rho \cos \theta \quad y = \rho \sin \theta$$

we have that

$$P(u, v) = \int_0^a \int_0^{2\pi} \exp(-i 2\pi(u \rho \cos \theta + v \rho \sin \theta)) \rho \, d\rho \, d\theta$$

where the limits of integration are across a circle of radius a . The circular aperture $p(x, y)$ is clearly circularly symmetric, so its Fourier transform must also be circularly symmetric. Therefore we only need to calculate $P(u, v)$ along one radial line, select the line with $v = 0$, to give

$$P(u, 0) = \int_0^a \int_0^{2\pi} \exp(-i 2\pi u \rho \cos \theta) \rho \, d\rho \, d\theta$$

Now from *Physical Mathematics* we have the standard identity that

$$\int_0^{2\pi} \exp(i r \cos \theta) \, d\theta = 2\pi J_0(r)$$



where $J_0(\rho)$ is the zero order Bessel function, we get that

$$P(u, 0) = 2\pi \int_0^a J_0(2\pi u \rho) \rho \, d\rho$$

We now need the second identity that

$$r J_0(r) = \frac{d}{dr} (r J_1(r)) \quad \text{so that} \quad \int_0^r J_0(t) t \, dt = r J_1(r)$$

so if we let $t = 2\pi u \rho$, we get that

$$P(u, 0) = \frac{1}{2\pi} \int_0^{2\pi u a} J_0(t) \frac{1}{u^2} t \, dt$$

which we can then integrate to get

$$P(u, 0) = \frac{2\pi u a}{u^2} J_1(2\pi u a) = 4\pi^2 a^2 \frac{J_1(2\pi u a)}{2\pi u a}$$

using that it is circularly symmetric, we can then write this in two dimensions as

$$P(u, v) = 4\pi^2 a^2 \frac{J_1(2\pi a w)}{2\pi a w} \quad \text{where } w^2 = u^2 + v^2$$



We then know from above that the intensity in the back focal plane of a lens of focal length f , is the square modulus of the Fourier transform scaled by λf , so giving,

$$I(s, t) = 4I_0 \left| \frac{J_1\left(\frac{2\pi}{\lambda f} a r\right)}{\frac{2\pi}{\lambda f} a r} \right|^2 \quad \text{where } r^2 = s^2 + t^2$$



where we have incorporated the various constants into I_0 , and is the intensity at the centre of the pattern.

To analyse this we need to consider the shape of the $J_1(x)/x$ and $|J_1(x)/x|^2$, both of which are plotted in figure 17. These functions have a similar shape to the $\text{sinc}()$ and $\text{sinc}^2()$, but have

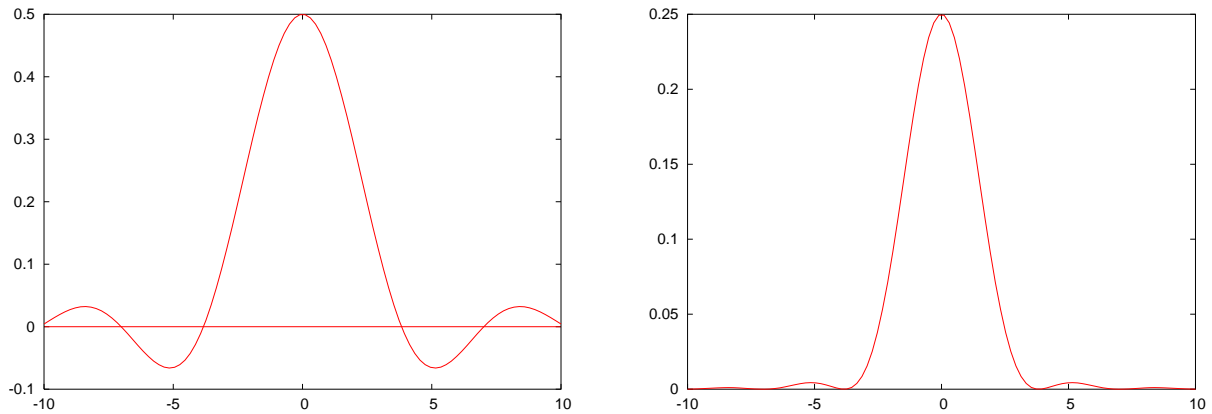


Figure 17: Plot of $J_1(x)/x$ and $|J_1(x)/x|^2$

1. Peak value of $J_1(x)/x$ at $x = 0$ is $1/2$.
2. Zeros located at x_0 , being:

x_0	3.832		1.22π
x_0	7.016		2.23π
x_0	10.174		3.24π
x_0	13.324		4.24π

3. Secondary maximas are lower than a sinc, or sinc^2 respectively.

The two dimensional function $|J_1(r)/r|^2$ is circularly symmetric and is plotted in figure 18 along with its $\log()$, which makes the ring patterns more obvious. This distribution is known as the *Airy Pattern*. The key feature of this pattern is the location of first zero, being at 1.22π .

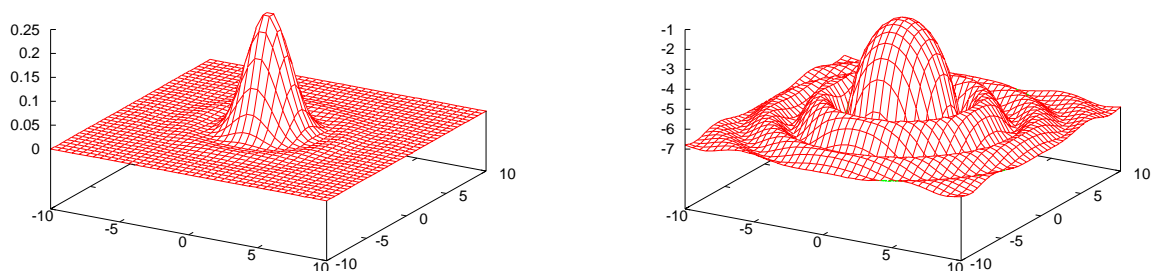


Figure 18: Two-dimensional surface plot of $|J_1(r)/r|^2$ and its $\log()$

If we have lens of focal length f and diameter d , then if we view a distant point object, the front of the lens will be illuminated by approximately plane waves. The aperture of the lens is circular, so in the back focal plane we will get a diffraction pattern from the

aperture. The distant object will therefore be imaged as the distribution $I(s, t)$ defines above as shown in figure 19. Note that a compound lens can be represented by a *simple* ideal lens located in the back principal plane. The key feature of this distribution is the

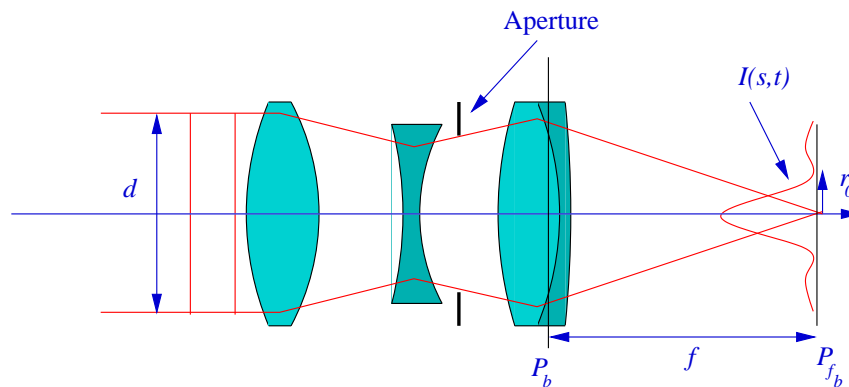


Figure 19: Point spread function of a lens

location of the first zero, being at radius,

$$r_0 = \frac{1.22 \lambda f}{2a} = \frac{1.22 \lambda f}{d} = 1.22 \lambda F_{No}$$



so is the same of all systems with the same F_{No} . This shows the image of a distant point object will be imaged as a bright central *spot* surrounded by a series of rings, known as the *Airy Rings*, the whole pattern being known as the *Point Spread Function* of the system.

2.8.1 Spatial Resolution of an Optical System

Just as the size of the grating limited the spectral resolution of a spectrometer, then the *Point Spread Function* limits the spatial resolution of an imaging system. If we consider *two* distant point object with angular separation $\Delta\theta$, then as shown in figure 20, in the back focal plane of an imaging system with focal length f , we get *two* point spread functions with, for *small* $\Delta\theta$, their peaks separated by

$$s = \Delta\theta f$$

There are three possible conditions, these being:

1. $s \gg r_0$ two well separated point spread functions, distant points are *resolved*.
2. $s \ll r_0$, the two point spread functions merge into one, and the distant points are *not resolved*,
3. $s \approx r_0$, there will be a *limit* where the distant points are *just resolved*.



There are a range of *resolution limits* the most useful and practical being the *Rayleigh Limit*, when $s = r_0$, so the peak of one point spread function at the zero of the other. This results in a *twin-peak* with a *dip* of about 20% between them as shown in figure 21.

In terms of *angular resolution*, we therefore get the *Rayleigh Limit* to be

$$\Delta\theta_0 = 1.22 \frac{\lambda}{d}$$

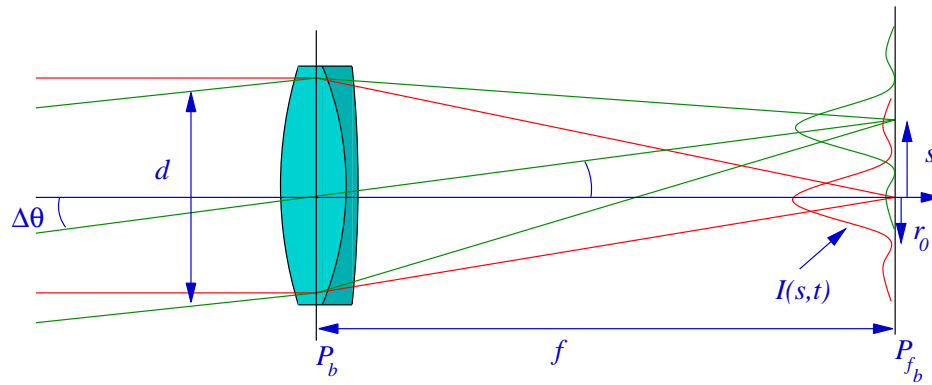


Figure 20: Image of two distant point objects.

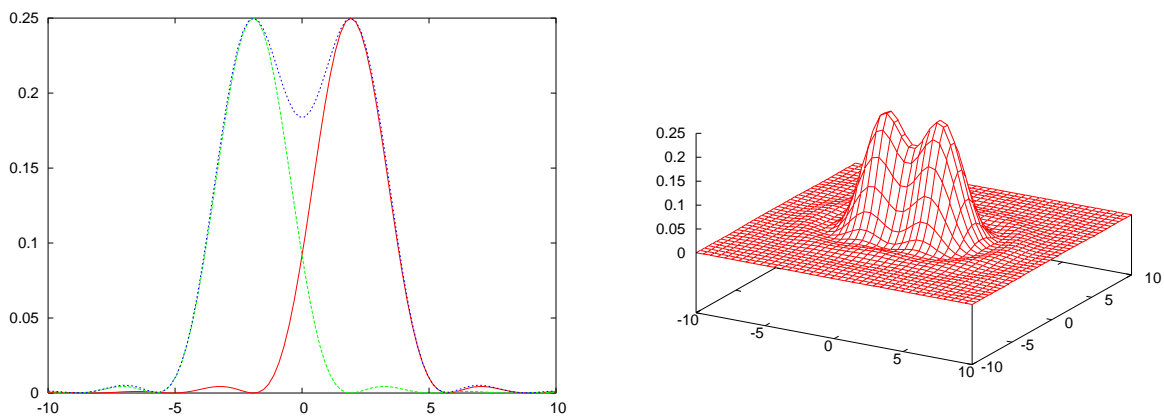


Figure 21: Plot of point spread functions at the Rayleigh resolution limit on one and two dimensions



so depends *only* of the diameter of the imaging system and the wavelength of light being imaged. This limit applies to a whole range of optical system, including the eye, telescopes, microscopes and cameras, see workshop questions for a range of numerical examples. This basic theory also applied to all other *waves* phenomena, including radar, microwaves, and even in acoustics!

When using this analysis for imaging system, for example a microscope, or camera, the image is not formed in the back focal plane, but rather in the image plane, a distance v from the back Principal plane, where v is given by the Gaussian Lens formula. Under these conditions, all the above analysis is still valid, by the scaling from Fourier Transform to diffracted intensity become λv rather than λf , see workshop question ?? for an example.

2.8.2 The Annular Aperture

Most large astronomical telescopes have fairly large central obstruction where the secondary mirror is located giving a annular aperture rather than a circular one. As in the previous sections, the diffraction pattern will be the scaled square modulus of the Fourier transform of the pupil, so we need to consider the Fourier transform of an annular aperture as shown in figure 22. This can be mathematically written as,

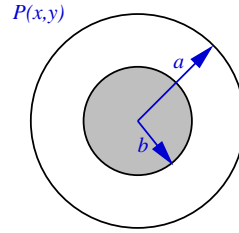


Figure 22: layout of an annular pupil.

$$p(x, y) = 1 \quad \text{for } a^2 < x^2 + y^2 < b^2 \\ = 0 \quad \text{else}$$

using polar coordinates as above, the Fourier transform of this is given by

$$P(u, v) = \int_a^b \int_0^{2\pi} \exp(-i 2\pi(u \rho \cos \theta + v \rho \sin \theta)) \rho \, d\rho \, d\theta$$

which only differs from the circular case in the limits of the radial integration. Again $p(x, y)$ is radially symmetric, so the Fourier transform will be radially symmetric. The angular integration is identical to the circular aperture, so that along one radial direction,

$$P(u, 0) = 2\pi \int_a^b J_0(2\pi u \rho) \rho \, d\rho = 2\pi \int_0^b J_0(2\pi u \rho) \rho \, d\rho - 2\pi \int_0^a J_0(2\pi u \rho) \rho \, d\rho$$

since $J_0()$ is a symmetric function.

This is just the difference between the Fourier transform of two circular apertures, one of radius b and one of radius a , so giving

$$P(u, v) = 4\pi^2 \left[b^2 \frac{J_1(2\pi b w)}{2\pi b w} - a^2 \frac{J_1(2\pi a w)}{2\pi a w} \right] \quad \text{where } w^2 = u^2 + v^2$$

The intensity of the point spread function is then just the scaled modulus squared of this, giving the rather complicated expression of

$$I(s, t) = B \left| b^2 \frac{J_1\left(\frac{2\pi}{\lambda f} b r\right)}{\frac{2\pi}{\lambda f} b r} - a^2 \frac{J_1\left(\frac{2\pi}{\lambda f} a r\right)}{\frac{2\pi}{\lambda f} a r} \right|^2 \quad \text{where } r^2 = s^2 + t^2$$

where the constant B is given by

$$B = \frac{4 I_0}{(b^2 - a^2)^2}$$

and I_0 is the intensity at the centre of the pattern.

The significance of this complicated expression only becomes apparent when it is plotted and compared to the intensity from an un-obstructed aperture of the same outer diameter as in figure 23, which is plotted for $a = 0.7b$.



The important features are:

1. Both have the basic shape with a large central peak and a series of secondary maximas.

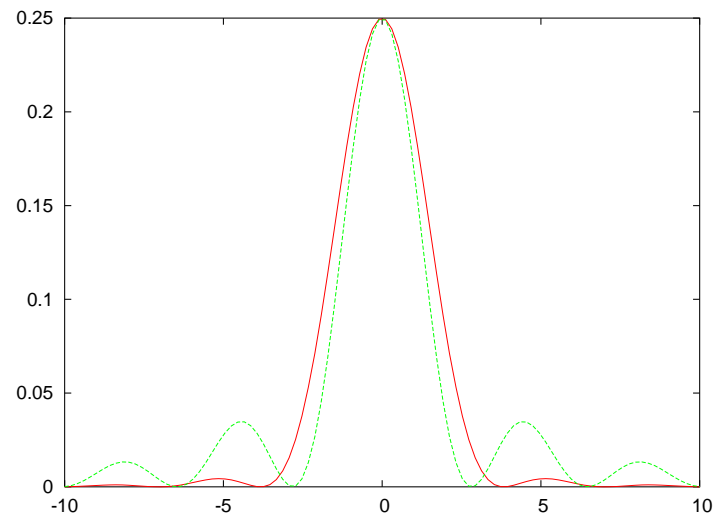


Figure 23: Comparison of annular point spread function with point spread function for un-obstructed aperture.

2. The secondary maximas for the obstructed aperture are *higher* than for the unobstructed case.
3. The central peak is *narrower* for the obstructed aperture, which is *not* what is expected.

A two-dimensional surface plot of the annular case shown in figure 24, shown the much more obvious ring pattern that than an unobstructed aperture in figure 18.

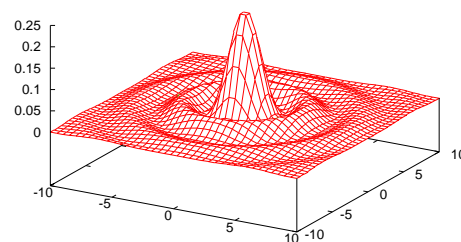


Figure 24: Surface plot of point spread function of an annular aperture with $a = 0.7b$.

As we have seen above, the angular resolution is for a telescope of focal length f is given by

$$\Delta\theta_0 = \frac{r_0}{f}$$

where r_0 is the radius of the first zero of the point spread function, so since the annular aperture has a narrow point spread function, its angular resolution will be smaller, so improved. This effect is shown graphically in figure 25, for an annular aperture with

$a = 0.7b$. The intensity distribution at the *Rayleigh* limit is plotted on the left, showing a very clear *dip*, so the points are well resolved. The plot on the right shown the stars separated by

$$\Delta\theta = \frac{\lambda}{d}$$

where they are still *resolved*. The actual resolution limit for the annular aperture does not have a simple analytical expression, but has to be found numerically, see workshop question ??.

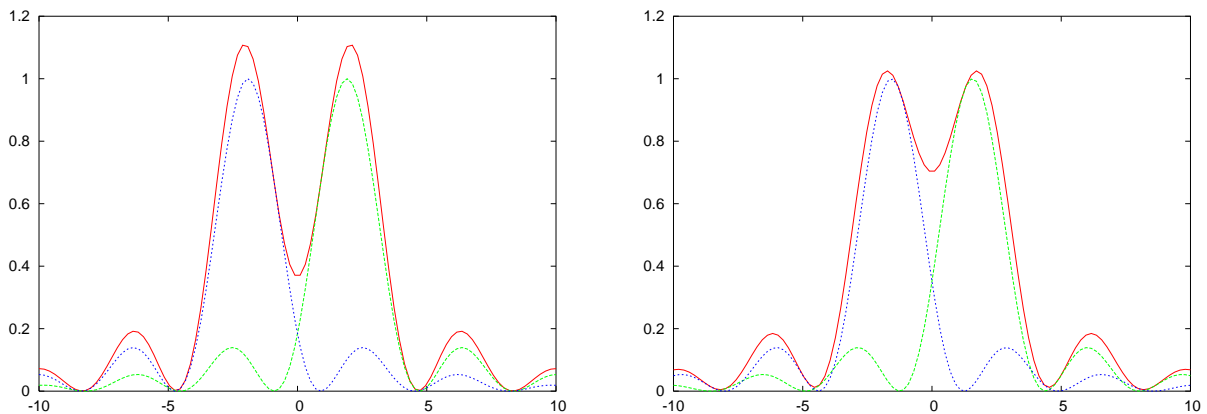


Figure 25: Plot of intensity distribution or annular aperture with two stars a) at the Rayleigh resolution criteria of $\Delta\theta = 1.22\lambda/d$ and b) below the Rayleigh criteria at $\Delta\theta = \lambda/d$

This improved resolution does have a cost, that being the absolute peak intensity which is proportional to the open area of the pupil which is clearly reduced by the presence of a central stop.

2.9 Resolution in Real Astronomical Telescopes

The above analysis assumes that a distant point source results in plane wavefronts across the input aperture of the system, with the resolution of the system limited only by diffraction. This is valid for *small* high quality system, for example microscopes, the human eye, small telescopes, and high quality camera systems; see workshop questions for numerical details. When we consider large astronomical telescopes, there is another very significant effect, that of the atmosphere. The refractive index of a gas depends on its local density, thus for air, it depends on pressure and temperature. Thus pressure and temperature gradients in the atmosphere result in local refractive index, and thus optical path length variations, as illustrated in figure 26. This is also why stars *twinkle*. As the atmosphere moves, this introduces a time varying phase aberration across the aperture of the telescope with the speed and extent of the variation depending on the local atmospheric conditions. This is known as the *seeing conditions*. In conditions of *good seeing*, the phase aberration can be considered constant for approximately $1/10^{\text{th}}$ of a second, and *plane* over a region, known as the *isoplanatic patch*.

Under these conditions, each *isoplanatic patch* acts as an individual telescope, with the

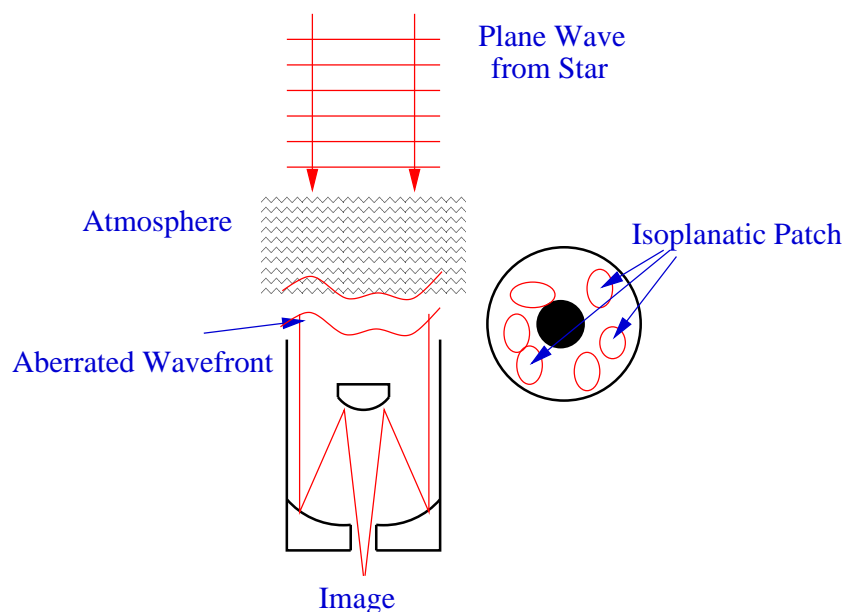


Figure 26: Schematic of a real terrestrial telescope.

*long exposure*². image of the star being an intensity summation of the image from each patch. The resolution is therefore limited by the size of the isoplanatic and not the overall aperture of the telescope. In areas of *good seeing*, the isoplanatic patch is 100 → 150 mm in diameter, giving an effective angular resolution of

$$\Delta\theta_e \approx 6 \times 10^{-6} \text{ Rad} \approx 1 \text{ sec of arc}$$

for $\lambda = 500 \text{ nm}$ and $d \approx 100 \text{ mm}$. Since the isoplanatic patches are time-varying, and not circular, then the shape of the point spread function will be time averaged, and will approximate a Gaussian with its radius, given by the e^{-2} intensity position, given, for a telescope of focal length f by approximately $\Delta\theta_e f$.

There are a range of schemes to minimise] this effect,

Telescope Location: Locate the telescope in areas of *good seeing*, typically high on a mountain plateau in an area of stable atmospheric conditions, Hawaii, Tenerife, Arizona are typical examples. The *ultimate* is to remove the atmosphere, hence the Hubble Space Telescope!

Short Exposures: Use exposure times *short* compared to the movement of the atmosphere, and combine after digital processing. Simplest scheme is to select the *sharp* images, align and average.

???

Adaptive Optics: Analyse the input distorted wavefront and correct its shape as shown in figure 27.

1. Part of the beam is split off and sent to a detector.
2. The shape of this distorted wavefront is analysed by a detector system, typically consisting of an array of *micro-lenses*.

²Long compared with the time constant of the atmosphere

3. The position on the image from each lens give the located gradient of the wavefront, so allowing the shape to be digitally reconstructed.
4. The wavefront shape is used set the to distort a *flexible* mirror, which typically think glass mirror that can be distorted by pizzo-electric stacks.
5. Reflected, corrected wavefront is split-off and used to for the image, free for the input aberration.
6. The wavefront sensing and correction run continuously at at rate comparable to the movement time of the atmosphere, typically $1/10^{\text{th}}$ second.

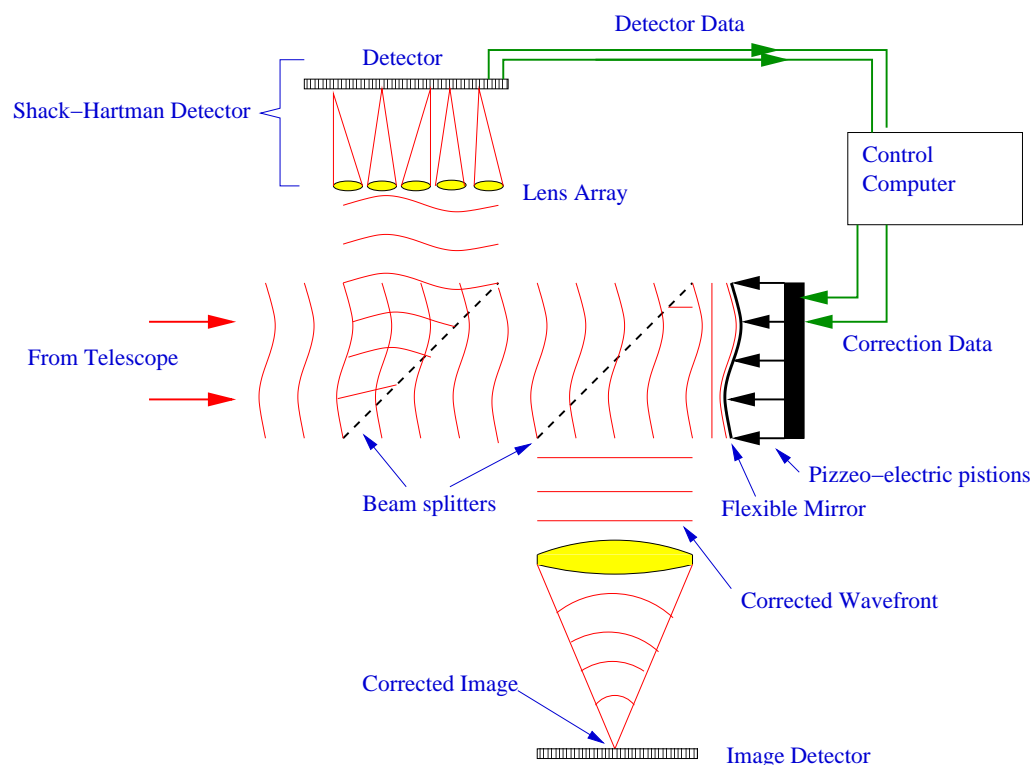


Figure 27: Layout of adaptive optical system for wavefront correction.

This system assume that there is a single bright *guide star* in the field of view which act as a point source, and hence a bright source of plane waves. The correction is then valid over the whole field of view so that dimmer objects close to the guide star are also corrected. This system gives significant improvement in resolution, and under optimal conditions, with a bright guide star can get within 20% of the Rayleigh diffraction limit of the full telescope aperture.

2.10 Summary

In this section we have,

1. Introduced the models in diffraction.
2. Diffraction from a single slit.

3. Diffraction from slit plus lens.
4. The Fourier Approach
5. Diffraction from Two Slits
6. The Diffraction Grating
7. The Grating Spectrometer
8. Practical Diffraction Gratings
9. Diffraction from Circular Aperture
10. Spatial Resolution in Optical Systems
11. The Annular Aperture
12. Resolution in real telescopes.